PHYSICS OF FLUIDS **19**, 086102 (2007)

Siloxanes: A new class of candidate Bethe-Zel'dovich-Thompson fluids

P. Colonna[a)]
Energy Technology Section, Department of Process and Energy, Delft University of Technology, Leeghwaterstraat 44, 2628 CA Delft, the Netherlands

A. Guardone
Dipartimento di Ingegneria Aerospaziale, Politecnico di Milano, Via La Masa 34, 20154 Milan, Italy

N. R. Nannan
Energy Technology Section, Department of Process and Energy, Delft University of Technology, Leeghwaterstraat 44, 2628 CA Delft, the Netherlands

(Received 15 February 2007; accepted 13 June 2007; published online 21 August 2007)

This paper presents a new class of Bethe-Zel'dovich-Thompson fluids, which are expected to exhibit nonclassical gasdynamic behavior in the single-phase vapor region. These are the linear and cyclic siloxanes, light silicon oils currently employed as working fluids in organic Rankine cycle turbines. State-of-the-art multiparameter equations of state are used to describe the thermodynamic properties of siloxanes and to compute the value of the fundamental derivative of gasdynamics Γ, whose negative sign is the herald of nonclassical gasdynamics. Siloxane fluids starting from D_6 and cyclic siloxanes of greater complexity, and MD_3M and linear siloxanes of greater complexity are predicted to exhibit a thermodynamic region in which Γ is negative and hence nonclassical wavefields are admissible. As an exemplary case, a nonclassical rarefaction shock wave propagating in fluid D_6 is studied to demonstrate the possibility of using siloxane fluids in nonclassical gasdynamic applications and to experimentally verify the existence of nonclassical wavefields in the vapor phase. The sensitivity of the present results to the considered thermodynamic model of the fluid is also briefly discussed. © *2007 American Institute of Physics*. [DOI: 10.1063/1.2759533]

I. INTRODUCTION

Most of the theory on gasdynamics is based on the ideal-gas law. It is well known, however, that even at moderate pressures (~1 bar) gaseous substances can exhibit an appreciable departure from ideal-gas behavior.[1] Therefore, in a relatively large thermodynamic region, the application of more complex equations of state (EoS) is mandatory. Real-gas flows can significantly differ, under both a qualitatively and quantitatively point of view, from their ideal-gas counterparts. The utilization of more complex thermodynamic models shows, for example, that compressible flows of fluids having a sufficiently large heat capacity may exhibit various interesting phenomena that are contrary to the predictions of the classical theory of gasdynamics. The property that governs the behavior of most compressible flows and, if negative, allows for unconventional gasdynamic phenomena to occur, is the fundamental derivative of gasdynamics, first introduced in this form by Hayes,[2] and defined as

$$\Gamma \equiv 1 + \frac{\rho}{c}\left(\frac{\partial c}{\partial \rho}\right)_s = \frac{v^3}{2c^2}\left(\frac{\partial^2 P}{\partial v^2}\right)_s. \qquad (1)$$

Here, ρ is the density, s denotes the entropy, P is the pressure, $v=\rho^{-1}$ is the specific volume, and c is the zero-frequency speed of sound $c^2=(\partial P/\partial \rho)_s$. Equation (1) shows that the fundamental derivative quantifies the variation of the speed of sound with density for isentropic transformations. For a polytropic (i.e., constant specific heat capacity) ideal gas, Γ is always greater than unity and shock waves of the compressive type only, are thermodynamically admissible. Even if real-gas behavior is taken into account and if the thermodynamic states are sufficiently far from the critical point, many substances consisting of simple molecules, e.g., air, N_2 (nitrogen), CH_4 (methane), etc., attain values of Γ that are always positive and consequently these substances admit only compression shock waves.[3] There is, however, no fundamental reason for Γ to be positive for all fluids in every thermodynamic state.[4,5] If the heat capacity of a fluid is sufficiently large and if real-gas behavior is at least qualitatively taken into account, Γ can become negative in a thermodynamic region adjacent to the saturated vapor line at high reduced pressures and temperatures.[4–6]

In the negative-Γ region of large-heat-capacity vapors nonclassical gasdynamic phenomena, including negative (rarefaction) shock waves are admissible.[7–12] Fluids that exhibit a dense-vapor thermodynamic region where $\Gamma < 0$ are referred to as BZT fluids in honor of Bethe, Zel'dovich, and Thompson for their contribution to the field of what is nowadays known as nonclassical gasdynamics. Apart from the numerous theoretical studies available in the scientific literature, no experimental evidence of nonclassical gasdynamic phenomena in the dense-vapor region is, however, currently available. In Ref. 13, Ivanov and Novikov report on the observation of rarefaction shock waves in solid iron and steel. In 1983, Borisov and co-workers[14] claimed to have observed a negative shock wave in chlorotrifluoromethane ($ClCF_3$, R-13) in close proximity to the critical point, where the initial state of the fluid and the state of the substance in the

---

[a)] Electronic mail: p.colonna@tudelft.nl wave itself were always in the single-phase region. This claim is restated by Kutateladze *et al.*[15] The results presented in Ref. 14, however, are confuted by Fergason *et al.*,[16] who show that the experiment by Borisov *et al.* is affected by critical point phenomena and two-phase effects (see also Ref. 17). Another experiment was conducted by Thompson *et al.*[18] to generate rarefaction shocks with phase transition. The last attempt known to the authors was an experiment using a shock tube;[19,20] the experiment aimed at the generation of a triple discontinuity exhibiting a nonclassical rarefaction shock in fluid PP10 ($C_{13}F_{22}$). Many problems were encountered however, ranging from incomplete rupture of the diaphragm, which complicated the measurement, and thermal decomposition of the working fluid with the formation of highly corrosive hydrofluoric acid (HF).

The lack of experimental evidence of nonclassical behavior in the vapor phase is due to many technical problems, including the identification of candidate BZT fluids among molecularly complex substances. Starting from the pioneering work of Lambrakis and Thompson,[21] many studies[22–25] relied upon various thermodynamic models to compute the value of Γ for several commercially available fluids in order to identify the most promising ones for both applications and experiments. The fluids under investigation were organic compounds and belong to the class of the alkanes, the ethers, the perfluorocarbons, and the siloxanes.

Due to their nontoxicity, excellent thermal and chemical stability, and limited flammability, siloxanes are possibly the most suitable fluids from an engineering point of view, if compared to the other classes of fluids. An added benefit of siloxanes is that these substances are already employed as working media in organic Rankine cycle engines (ORCs)[26] and are proposed for promising ORC applications.[27–29] The ORC engine is one the applications that in principle can benefit from BZT phenomena.[30] The isentropic efficiency of these turbines can in principle be increased if they are operated with BZT fluids, and if the expansion process is carried out, even partially, in the nonclassical gasdynamic region. As a result of the adoption of a heavy organic fluid, the speed of sound is low, therefore ORC turbines operate in the transonic or supersonic regime. Consequently, compression shock waves are an often occurring but unwanted phenomenon. Moreover, due to the strong adverse pressure gradient created by the compression shock, boundary layer detachment becomes a problem resulting in a significant loss of lift and potential to extract work from the working fluid. A number of studies shows that in principle it is possible to obtain a shock-free flow in the stator if the thermodynamic state at the stator inlet is appropriately chosen.[24,30–33]

In this paper, following the same line of Cramer, who in 1989 studied the BZT character of perfluorocarbons,[23] one of the most accurate thermodynamic models currently available is used to investigate the existence and extension of the negative-Γ region of siloxanes.

Estimates of Γ, which are relevant for the experimental identification of BZT fluids and for designing processes involving nonclassical gasdynamic phenomena, are not trivial. The main difficulty is that the accuracy of calculations of derived thermodynamic functions, and therefore of Γ, very much depends on the functional form of the thermodynamic model, the accuracy of the data (e.g., critical properties, saturation data, P-ρ-T data, etc.) on which the model is based, and on the accuracy and functional form of the ideal-gas heat capacity correlation, as discussed in Sec. III A. This is especially true within the region where the fundamental derivative may become negative, i.e., $0.75 < P/P_c < 1$, $0.96 < T/T_c < 1.01$, and $1.4 < v/v_c < 2.5$ (subscript c indicates the critical point value).[34] Moreover, it is worthwhile recalling that presently the amount of experimental thermodynamic data for heavy/complex substances, e.g., critical properties and ideal-gas heat capacities, are scarce because experimental conditions pose many technical problems. For example, critical properties must be measured at quite high temperatures, close to the thermal stability limit of the fluid, and, due to the low volatility of heavy fluids, measurements at ambient temperatures (or higher) need to be performed at close to vacuum conditions.

In this study, the fundamental derivative and other thermodynamic properties of siloxanes are computed from the recently developed Span-Wagner (SW) multiparameter functional form for nonpolar substances.[35] The substance-specific parameters of the Span-Wagner equation were recently determined by Colonna and co-workers.[36] This functional form has been chosen because (i) it has qualitatively correct extrapolation behavior, even outside the range where the equation is fit to experimental data;[35] (ii) due to its optimized functional form, one single thermodynamic model can accurately and consistently predict thermodynamic properties for both nonclassical gasdynamics calculations and for process design; and (iii) its accuracy can always be improved whenever more experimental data become available. The present study complements the preliminary results on siloxanes discussed in Ref. 24, obtained using the Peng-Robinson-Stryjek-Vera (PRSV) equation of state.[37,38]

This paper is organized as follows. Section II presents a brief review regarding fluids that were predicted to exhibit a negative-Γ region; i.e., BZT fluids. Section III summarizes the main physical characteristics of siloxanes and gives a short overview of the multiparameter EoS adopted to model the fluids. In Sec. III B the computation of Γ in the dense-vapor thermodynamic region is presented for several cyclic and linear siloxanes. The fluids of the siloxane family for which a negative-Γ region is computed with the chosen thermodynamic model are put into evidence and the results are discussed. As an exemplary application, the case of a nonclassical rarefaction shock wave propagating in fluid D_6 is also presented. Finally, Sec. IV gives some concluding remarks and a summary.

II. CRITICAL EVALUATION OF CANDIDATE BZT FLUIDS

Tracking down a class of fluids that may exhibit nonclassical gasdynamic behavior and which can be used in practical applications is to be based on several considerations. First, a number of fluid parameters related to the strength of potential BZT effects must be assessed; e.g., the dimensionless ideal-gas heat capacity C_v^0/R.[25] Equally important con-

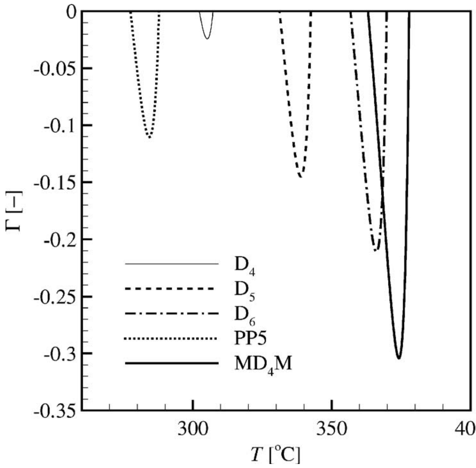

FIG. 1. Γ along the saturated vapor line for several siloxanes and a perfluorocarbon. Thermodynamic properties are computed using the PRSV EoS (Refs. 37 and 38).

siderations are the availability of thermophysical property data, fluid characteristics, e.g., thermal decomposition temperature, fluid availability and price, and safety concerns such as toxicity and flammability. These evaluation criteria are intimately linked: the strength of nonclassical gasdynamic effects is related to the capacity of the molecule to store energy; i.e., to its specific heat.[12] However, depending on the fluid class, a more complex structure of the molecule can result in a lower thermal stability. Furthermore, high temperature is closely related to the risk of explosion and thermal decomposition can be the cause of the formation of toxic gases.

Currently three classes of fluids are believed to exhibit a $\Gamma < 0$ region in the vapor phase; namely, hydrocarbons,[21,22] perfluorocarbons,[21,23,25] and siloxanes.[24] Any application exploiting nonclassical gasdynamic effects would involve high temperatures therefore complex hydrocarbons which could potentially exhibit BZT effects, such as n-decane,[21] would pose very difficult technical problems because of the risk of explosion. Complex perfluorocarbons are potentially very attractive because they have a lower critical temperature with respect to siloxanes and a very complex molecular structure which entails high values of C_v^0/R and low values of Γ. The comparably lower critical temperature of perfluorocarbons implies that the BZT region is located at lower temperatures. As an example, Fig. 1 shows the negative-Γ values along the dew-line of D_4 [octamethylcyclotetrasiloxane, $((CH_3)_2SiO)_4$], D_5 [decamethylcyclopentasiloxane, $((CH_3)_2SiO)_5$], D_6 [dodecamethylcyclohexasiloxane, $((CH_3)_2SiO)_6$], and PP5 [perfluorodecalin, $C_{10}F_{18}$] as calculated by the Peng-Robinson-Stryjek-Vera (PRSV) equation of state[37,38] (PRSV EoS). Perfluorocarbons are also known to be extremely thermally stable among organic fluids. Assuming that siloxanes and perfluorocarbons have similar thermal stability, the safety margin with respect to decomposition would be greater for perfluorocarbons.

On the other hand, decomposition products of perfluorocarbons are highly aggressive, e.g., hydrofluoric acid (HF) and possibly other very toxic compounds, whereas thermal decomposition of siloxanes leads to polymerization and the polymer product is not toxic.

Moreover, the knowledge of the thermophysical properties of perfluorocarbons is at a far lower stage if compared to siloxanes and this makes the design of any experiment or application and the setting of the operating conditions much more problematic. The thermodynamic modeling of siloxanes is instead in an advanced stage[36] and their thermal stability in conditions similar to the foreseen experiment has been tested already.[39,40] Furthermore, flammability of siloxanes is much lower than that of hydrocarbons. The simpler molecules of the siloxanes' class are currently utilized in organic Rankine cycle turbines, which is the first application proposed for the exploitation of BZT effects.[30]

All the mentioned reasons put into evidence that at the moment siloxanes are possibly the best class of fluids for experiments and applications involving nonclassical gasdynamic phenomena.

III. SILOXANES

Siloxanes are a class of fluids composed of molecules containing alternate silicon and oxygen atoms in either a linear or cyclic arrangement usually with two or three organic groups attached to each silicon atom. Figures 2(a)–2(c) show the geometry of three exemplary siloxanes as computed by recent *ab initio* calculations performed to determine the isobaric specific heat in the ideal-gas state.[41] At ambient conditions, siloxanes are liquid and appear slightly viscous, odorless, and transparent. For this work, the cyclic molecules D_4 (octamethylcyclotetrasiloxane, $C_8H_{24}O_4Si_4$), D_5 (decamethylcyclopentasiloxane, $C_{10}H_{30}O_5Si_5$), and D_6 (dodecamethylcyclohexasiloxane, $C_{12}H_{36}O_6Si_6$) together with the linear molecules MDM (octamethyltrisiloxane, $C_8H_{24}O_2Si_3$), MD_2M (decamethyltetrasiloxane, $C_{10}H_{30}O_3Si_4$), MD_3M (dodecamethylpentasiloxane, $C_{12}H_{36}O_4Si_5$), and MD_4M (tetradecamethylhexasiloxane, $C_{14}H_{42}O_5Si_6$) were selected. In Table I, relevant thermophysical properties of linear and cyclic siloxanes are reported.

In principle, these siloxanes can all be used as working fluids in organic Rankine cycle turbines depending on the power level: the optimization of the cycle for the working fluid points to molecules with higher complexity for lower power output and vice versa.

A. Multiparameter EoS for siloxanes

Numerous theoretical[4–6] and numerical studies[42–46] on nonclassical gasdynamics are based on the simple polytropic Van der Waals cubic EoS. However, it is well known that relevant thermodynamic data obtained from the Van der Waals EoS are highly inaccurate, even more so for the fundamental derivative, which requires the computation of first and second-order derivatives of the equation of state. This is illustrated by expanding Eq. (1) as

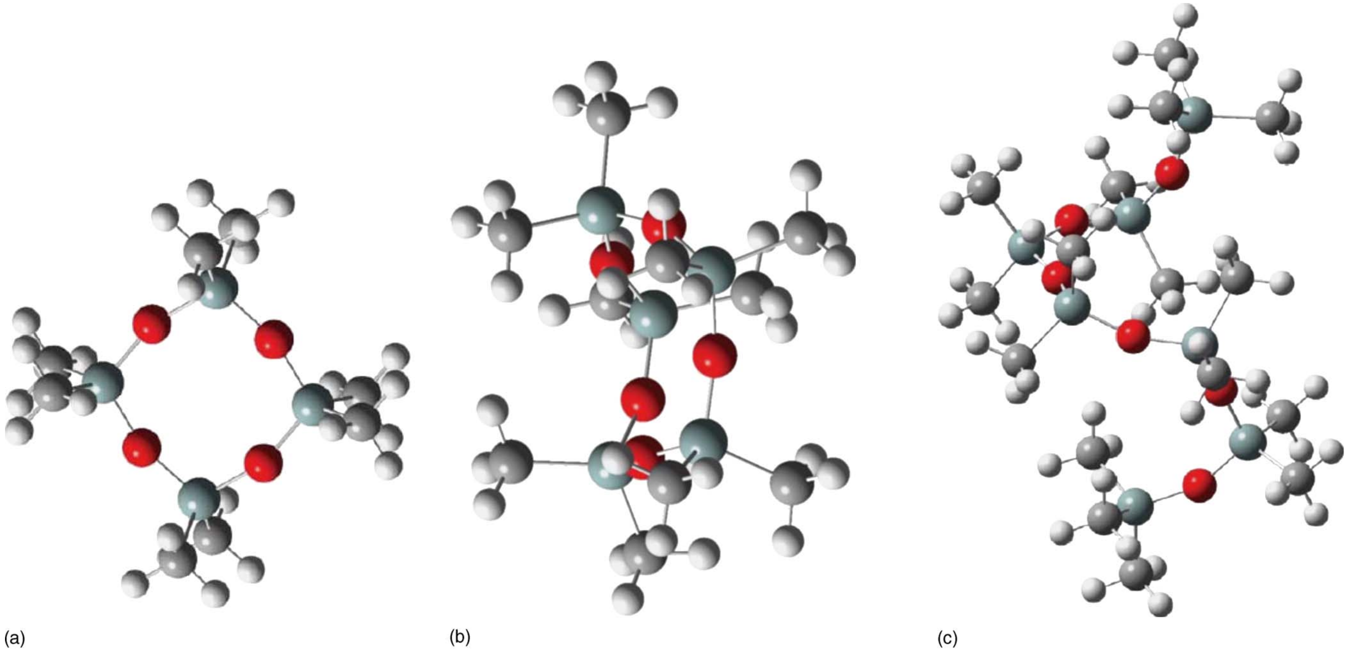

FIG. 2. (Color online) Molecular structure of two cyclic and one linear siloxane. The optimized geometries are taken from Ref. 41. (a) D_4; (b) D_5; (c) MD_5M.

$$\Gamma = \frac{v^3}{2c^2}\left(\left(\frac{\partial^2 P}{\partial v^2}\right)_T - 3\frac{T}{C_v}\left(\frac{\partial P}{\partial T}\right)_v\left(\frac{\partial^2 P}{\partial v\,\partial T}\right) + \left[\frac{T}{C_v}\left(\frac{\partial P}{\partial T}\right)_v\right]^2 \times\left\{3\left(\frac{\partial^2 P}{\partial T^2}\right)_v + \frac{1}{T}\left(\frac{\partial P}{\partial T}\right)_v\left[1-\frac{T}{C_v}\left(\frac{\partial C_v}{\partial T}\right)_v\right]\right\}\right), \qquad (2)$$

where T is the temperature and C_v is the isochoric heat capacity of the fluid.

Recent studies on BZT fluids therefore relied on more complex EoS, including the Peng-Robinson-Stryjek-Vera EoS[24,31,47,48] and the Martin-Hou (MH) EoS.[19,34] The latter, derived to describe the thermodynamic properties of freon-13, has been chosen in the case of perfluorocarbons because of its accuracy in predicting the thermodynamic properties of (lighter) fluorocarbons. Remarkably enough, due to the scarcity of thermodynamic data in the alleged negative-Γ region,[49] all these models have not been validated and the accuracy of the obtained results is questionable.[25]

To comply with the demanding constraints on the accuracy of the thermodynamic model, equations of state in the Span and Wagner functional form[35] are adopted in the present work. The correlation developed by Span and Wagner is a multiparameter function where the reduced Helmholtz energy, i.e., $\psi \equiv \Psi/(RT)$, is expressed as a function of the reduced density, $\delta \equiv \rho/\rho_c$, and the inverse of the reduced temperature $\tau \equiv T_c/T$. The functional form depends on 12 substance-specific parameters $n_1, \ldots, n_{12}$ and reads

$$\begin{aligned}\psi(\tau,\delta) &= \psi^0(\tau,\delta) + \psi^r(\tau,\delta)\\ &= \psi^0(\tau,\delta) + n_1\delta\tau^{0.250} + n_2\delta\tau^{1.125} + n_3\delta\tau^{1.500}\\ &\quad + n_4\delta^2\tau^{1.375} + n_5\delta^3\tau^{0.250} + n_6\delta^7\tau^{0.875}\\ &\quad + n_7\delta^2\tau^{0.625}e^{-\delta} + n_8\delta^5\tau^{1.750}e^{-\delta} + n_9\delta\tau^{3.625}e^{-\delta^2}\\ &\quad + n_{10}\delta^4\tau^{3.625}e^{-\delta^2} + n_{11}\delta^3\tau^{14.5}e^{-\delta^3}\\ &\quad + n_{12}\delta^4\tau^{12.0}e^{-\delta^3}. \qquad (3)\end{aligned}$$

Here, ψ^0 represents the ideal-gas contribution to the Helmholtz free energy (see the Appendix), and it is obtained from an ideal-gas heat capacity correlation, and ψ^r accounts for the difference between real-gas and ideal-gas behavior. Equation

TABLE I. Relevant thermophysical property data for the linear and cyclic siloxanes considered in this study. MW is the molecular weight, T_c, P_c, and v_c the critical temperature, pressure, and volume, respectively, T_{TP} is the temperature at the triple point, T_{NBP} is the temperature at the normal boiling point, and ω is the acentric factor. The value of ω is computed from its definition (see, e.g., Ref. 59) using the vapor-pressure predictions of the SW EoS.

Fluid name	MW [kg/kmol]	T_c [K]	P_c [kPa]	v_c [$\mathrm{m}^3/\mathrm{kmol}$]	Z_c [-]	T_{TP} [K]	T_{NBP} [K]	ω [-]
MDM	236.53	564.1	1415.2	0.921	0.278	187.15	425.7	0.530
MD_2M	310.69	599.4	1179.4	1.196	0.283	205.15	467.4	0.650
MD_3M	384.84	628.4	945.0	1.458	0.264	192.00	503.0	0.722
MD_4M	458.99	653.2	877.5	1.607	0.260	214.15	532.7	0.825
D_4	296.62	586.5	1332.0	0.958	0.262	290.25	448.5	0.593
D_5	370.77	619.2	1160.0	1.267	0.286	235.15	484.1	0.658
D_6	444.92	645.8	961.0	1.594	0.285	270.15	518.1	0.736

TABLE II. Comparisons among the performance of the Peng-Robinson-Stryjek-Vera (PRSV), Martin-Hou (Ref. 51) (MH), and Span-Wagner (SW) EoS regarding the prediction of experimental thermodynamic data of MDM. The performance is assessed by means of the average absolute deviation of experimental data with respect to computed values.

Property	Source	P range [bar]	T range [K]	DEV [%]		
				PRSV	MH	SW
ρ^L	Lindley and Hershey (Ref. 60)	—	426–564	8.04	3.11	0.42
	Hurd (Ref. 61)	—	273–333	0.83	—	0.15
ρ^V	Lindley and Hershey (Ref. 60)	—	460–564	1.66	15.87	0.87
P^{sat}	Flaningam (Ref. 62)	—	346–436	0.54	99.90	0.06
	Lindley and Hershey (Ref. 60)	—	322–564	1.08	0.34[a]	0.41
	Skorokhodov *et al.* (Ref. 63)	—	344–418	9.76	—	9.62
P-ρ-T	Marcos *et al.* (Ref. 64)	0.36–3.77	448–573	2.51	1.78	0.60
	McLure *et al.* (Ref. 65)	1.01325	300–412	0.78	Predicts vapor	0.01

[a] $525 < T < 564$; for lower temperatures, the average absolute deviation increases significantly to approximately 36% at $T=480$ K.

(3) is valid for many classes of nonpolar and weakly polar fluids and it was developed by means of an optimization algorithm that considered data sets for different fluids and fluid families simultaneously. The correct extrapolation behavior of the established equation was taken into consideration in the development phase. Peculiar features of Eq. (3) are the following:

(1) The functional form is defined by relatively few parameters and allows for numerically stable and consistent predictions of thermodynamic data over the entire range of interest for advanced technical applications, therefore one and the same fundamental equation can be used for process computations and for nonclassical gasdynamic simulations. Remark that the objective of Span and Wagner was to develop a functional form which provided the best equation based on the data used for its development and not just the best fit of the data.

(2) The 12 parameters can be determined from a restricted set of experimental data; furthermore Span and Wagner[35] illustrate for n-octane that, due to its optimized functional form, the thermodynamic model can be used to predict thermodynamic data which are qualitatively correct outside the range where experimental information is available (see also Ihmels[50]). Since the siloxanes also have a complex molecular structure, just like n-octane, it can be expected that the extrapolation behavior of the established thermodynamic models for the selected siloxanes[36] is good. Note that the correct behavior of the EoS was taken into account by Span and Wagner in the development phase of the functional form.

(3) Once the Span-Wagner fundamental equation for a substance is established, it can always be improved when additional and/or more accurate experimental data become available.

The Appendix provides relevant equations for computing Γ from a standard Helmholtz function; e.g., Eq. (3).

A recent study documents the development of such thermodynamic models for siloxanes[36] and demonstrates the superior performance if compared to simpler equations of state. The reduced ideal-gas Helmholtz energy ψ^0 has been calculated using a simple polynomial correlation; i.e.,

$$C_P^0(T) = \alpha + \beta T + \gamma T^2 + \epsilon T^3. \qquad (4)$$

The substance-specific parameters α-ϵ were determined by fitting Eq. (4) to data reported in Ref. 41, which were obtained from speed-of-sound measurements and *ab initio* calculations. The ideal-gas isobaric heat capacity correlation is valid for temperatures between 273 and 673 K. Note that extrapolation outside this temperature range leads to inaccurate results. The maximum temperature is limited by the fluid's decomposition temperature. The 12 parameters of Eq. (3) have been obtained by fitting the functional form to selected experimental and estimated data, using appropriate weights, as documented in Ref. 36. To do this effectively, a multiproperty fitting algorithm developed at NIST, was used. For D_4, D_5, and MD_4M, the 12 parameters are reported in Ref. 36; the results for MDM, MD_2M, MD_3M, and D_6 are documented in a manuscript submitted for publication. A comparison of the accuracy in estimating thermodynamic properties for MDM among the Span-Wagner, Peng-Robinson-Stryjek-Vera, and Martin-Hou[51] equations of state is reported in Table II. The results show that the performance of the SW EoS in predicting thermodynamic data in the dense vapor phase, the region of interest for nonclassical gasdynamics, is superior to that of the PRSV EoS to a certain extent. The MH EoS seems inadequate for the estimation of primary properties such as the saturated vapor density and pressure, therefore even more so for a secondary property such as Γ.

B. The nonclassical region of siloxanes

Table III lists the minimum value of Γ along the saturated vapor line as computed from the EoS in the Span-

TABLE III. Minimum value of Γ along the dew-line. Values are calculated with the newly developed equations of state (Ref. 36) in the Span-Wagner functional form for nonpolar fluids and with the PRSV EoS.

	Γ^V_{min}	
Fluid	SW	PRSV
MDM	0.085	0.037
MD_2M	0.074	−0.013
MD_3M	−0.091	−0.271
MD_4M	−0.086	−0.304
D_4	0.087	−0.024
D_5	0.050	−0.145
D_6	−0.220	−0.307

Wagner functional form and the PRSV EoS. The minimum value along the saturated vapor line is also the minimum value in the vapor phase. The results show that D_6, MD_3M, and MD_4M are BZT fluids, since they have $\Gamma^V_{\text{min}} < 0$. Figure 3(a) shows the coexistence curve and the $\Gamma = 0$ line computed according to the PRSV, and Martin-Hou equations of state for D_4; the SW EoS does not predict a negative value for Γ in the dense vapor region. The regions of negative nonlinearity are also put into evidence in Figs. 4 and 5, where iso-Γ-lines are presented in a *P*-*T* plane for all remaining siloxane fluids. These *P*-*T* diagrams provide preliminary information about the process conditions which would be involved either in the design of a BZT experiment[34,47] or in any application exploiting nonclassical gasdynamic phenomena.

Compared to previous work,[21–25] the shape of the region delimited by the iso-Γ-line and the dew-line is similar. This gives assurance that the results obtained from the Span-Wagner functional form are consistent. Moreover, the smaller is Γ^V_{min}, the larger the size of the so-called region of negative nonlinearity ($\Gamma < 0$ region).

The two-parameter principle of corresponding states may be used within each family, i.e., for linear and cyclic siloxanes separately, with sufficient confidence. Application of the two-parameter principle of corresponding states then suggests that linear and cyclic siloxanes of greater complexity are also BZT fluids; e.g., MD_5M and D_7. According to the same theory and to the conclusions presented in Ref. 34, Γ^V_{min} diminishes as molecular complexity increases, as can be observed in Table III, with only the exception of fluid MD_4M. This can be explained by the fact that several uncertainties affect the accuracy of the adopted thermodynamic models for this fluid and therefore the calculation of Γ. First, the critical point data on which the equations of state depend are inconsistent within this family (see Table I). Critical data were selected among various sources[36] that were critically evaluated, even though the problem of inconsistency could not be solved yet due to the scarcity of experimental information. Other major sources of uncertainty are the unavailability of dense-vapor *P*-ρ-*T* data and saturation data.

In the following section, the uncertainty related to the errors in the prediction of the isochoric heat capacity of the fluids in the dilute gas limit is investigated.

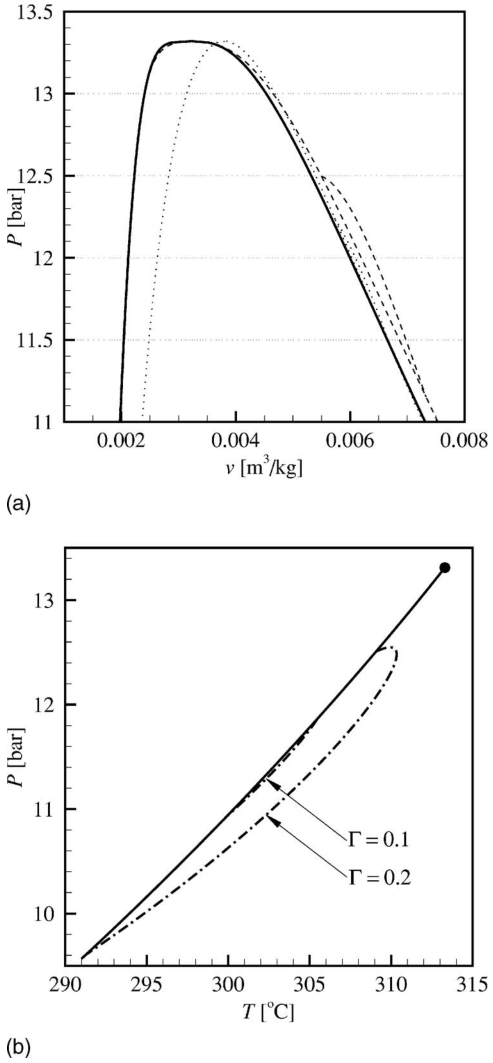

FIG. 3. (a) The region of negative nonlinearity in the *P*-*v* thermodynamic plane of D_4 as predicted by the PRSV (···) and MH EoS (---). The Span-Wagner EoS (—) does not predict a region of negative nonlinearity. (b) Iso-Γ-lines in the *P*-*T* plane of D_4 obtained from the Span-Wagner EoS. (●) Critical point.

C. Sensitivity to the ideal-gas specific heat capacity

Although for linear and cyclic siloxanes there are enough data to develop Span-Wagner type EoS,[36] for the most complex molecules of the two classes, there are currently no experimental *P*-ρ-*T* data and no saturation data at the high reduced temperatures and pressures where the BZT region can be located. A complete uncertainty analysis on the value of Γ is therefore not possible. It is, however, possible to analyze the sensitivity of the value of Γ to the uncertainty in C^0_P; the substance-specific parameters of the ideal-gas C^0_P correlation equation (4) are determined by fitting the equation to C^0_P data obtained from *ab initio* calculations[52] relying on several sound speed measurements that were recently conducted.[53] The predicted ideal-gas heat capacities from *ab initio* computations have an estimated uncertainty of about 5%. Taking the uncertainty of 5% into account, Table IV indicates the sensitivity of Γ_{min} along the dew-line. The values of Γ_{min} calculated with the Span-Wagner EoS indicate

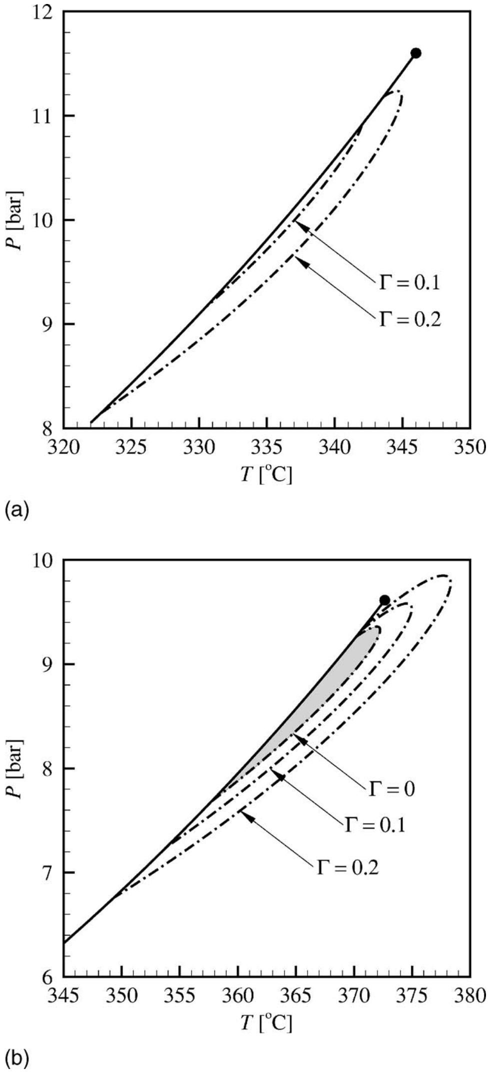

FIG. 4. Iso-Γ-lines in the P-T plane for cyclic siloxanes. Thermodynamic properties are obtained from the Span-Wagner EoS. (●) Critical point. The shaded area represents the $\Gamma < 0$ region. (a) D_5; (b) D_6.

that the uncertainty on the value of C_P^0 does not affect the sign of $\Gamma_{\min}$ for any of the considered fluids.

D. A rarefaction shock wave in fluid D_6

As an exemplary case of nonclassical gasdynamic behavior in siloxane fluids, the propagation of a rarefaction shock wave in fluid D_6 is simulated numerically. The test case is related to a project at the Energy Technology section of the Delft University of Technology that aims at the generation and detection of a rarefaction shock wave in the dense-gas region of a siloxane. The shock wave is generated in the charge part of a Ludwieg tube operated with a fast-opening valve. A nozzle is interposed between the high-pressure and the low-pressure parts in order to avoid the propagation of disturbances from the plenum back into the test section. In total, the length of the Ludwieg tube is 11.15 m and the diameter of the pipe is 100 mm. Figure 6 shows the simplified geometry adopted for the simulation.

The initial state in the high-pressure tube is set to 912.62 kPa and 369.19 °C. This state is in the superheated dense vapor region, close to saturation and characterized by a negative value of Γ. The ratio of the area of the throat with respect to the area of the pipe, i.e., A^*/A, is computed such as to (i) guarantee that, for a given high-pressure state in the pipe, the nozzle operates under choked conditions and (ii) that the generated expansion wave is a single rarefaction shock and not a mixed nonclassical wave composed by a leading shock followed by an isentropic rarefaction wave. With this initial state it is found that $A^*/A = 0.4196$ and that in the throat the pressure and temperature are 557.40 kPa and 357.35 °C, respectively (Table V). The pressure in the vessel is set to 500.00 kPa and the temperature is set to the same value as for the fluid in the pipe; i.e., 369.19 °C. Since the pressure in the vessel is lower than the pressure in the throat of the nozzle, the flow through the nozzle is choked. For the simulation, the fast-opening valve is idealized as a diaphragm disappearing instantaneously at $t = 0$ s. Its position is at 10 cm downstream the throat of the nozzle. The mesh distribution in the pipe on the left is uniform, although near the nozzle the mesh changes smoothly from a coarse distribution to a fine distribution. In total, 1669 cells were used. The numerical solution is obtained with a quasi-one-dimensional Euler solver[31] in which thermodynamic properties of D_6 are calculated with the SW EoS. The same equation of state is used also in the analytical computations of which the results are reported in Table V.

Figure 7(a) shows, in the P-v plane, the pre- and post-shock states and the expansion of the fluid from the post-shock state up to the nozzle throat. Figure 7(b) gives the results of the numerical simulation; namely, the pressure and the absolute Mach profile at $t \approx 130$ ms. The expansion waves satisfies the Rankine-Hugoniot jump conditions and it is therefore a single rarefaction shock wave. The nonclassical rarefaction shock wave has a pressure drop of the order of 1 bar, propagating slightly supersonically ($\mathrm{Ma} = 1.02$) into the quiescent medium in the pipe.

Note that the effects of the shear and bulk viscosity and the thermal conductivity are neglected. As a consequence of these assumptions, the shock internal structure and the interaction between the shock and the boundary layer behind the shock, which reduces the shock intensity, cannot be taken into account.

The mentioned simplifications lead to several considerations. For the weak nonclassical shock considered here, reduction of the shock intensity due to the growth of the boundary layer is not significant.[48,54] The boundary layer which develops behind the shock, is a laminar region (see Mirels[55]). Using a similarity between the flow through the Ludwieg tube with that due to an impulsively moved flat plate,[3] the thickness of the (laminar Blasius) boundary layer can be determined from

$$\frac{\delta(\bar{x})}{\bar{x}} \approx 4.9 \sqrt{\frac{\mu}{\rho u \bar{x}}}, \tag{5}$$

where $\delta(\bar{x})$ denotes the thickness of the boundary layer at a distance $\bar{x}$ measured from/behind the shock, μ is the dynamic viscosity at the postshock state, and ρ and u are the post-shock density and absolute fluid velocity, respectively. If the

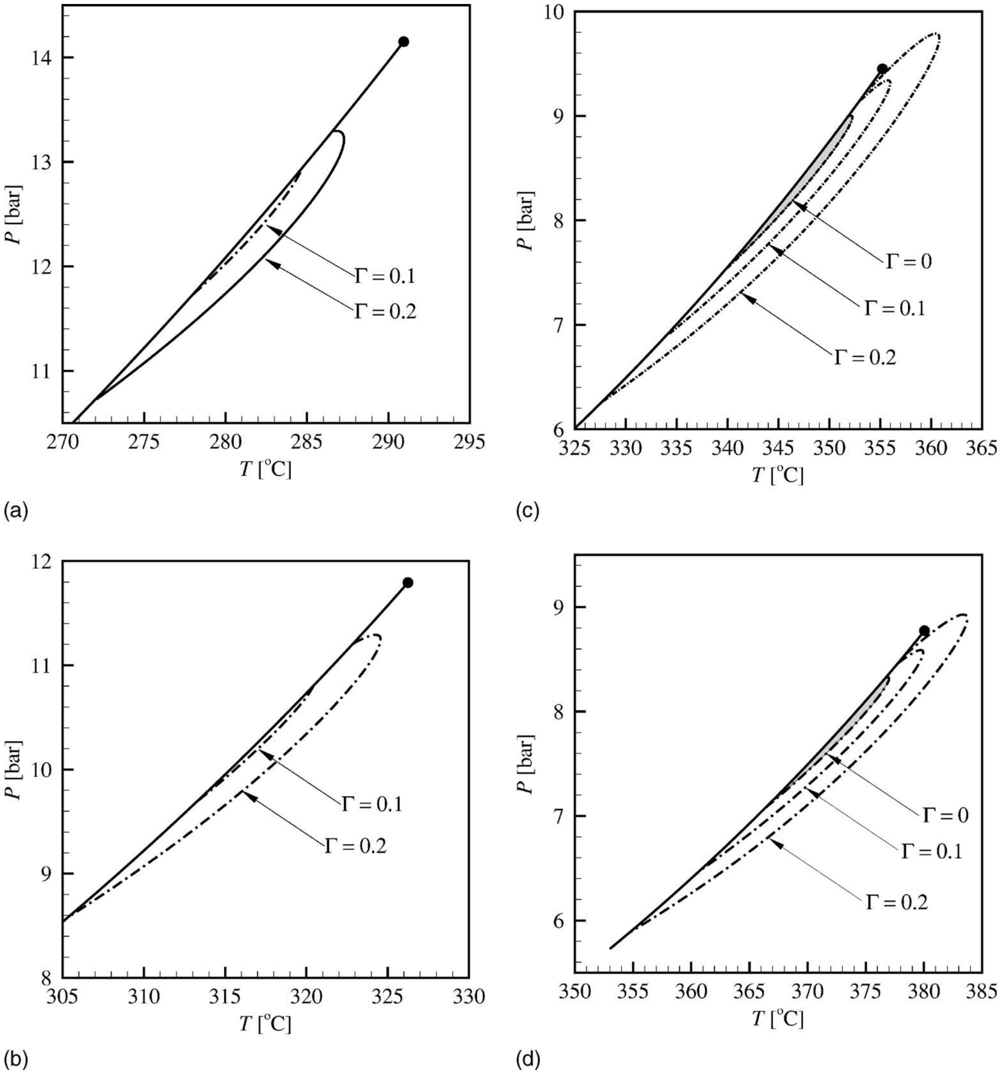

FIG. 5. Iso-Γ-lines in the *P-T* plane for linear siloxanes. Thermodynamic properties are obtained from the Span-Wagner EoS. (●) Critical point. The shaded area represents the $\Gamma < 0$ region. (a) MDM; (b) MD_2M; (c) MD_3M; (d) MD_4M.

viscosity is computed using the method of Chung *et al.*[56] at the postshock state (see Table V), it is found that $\mu = 1.74 \times 10^{-5}$ Pa/s and $\delta(\bar{x})/\bar{x} = 0.44 \times 10^{-3}$ or equivalently, $\delta(10\ \text{m}) = 4.4$ mm.

Points for further discussion are the possibility that dispersion of the rarefaction shock occurs due to thermal relaxation within the shock front, and that a region of nonequilibrium may exist behind the shock, also because of thermal relaxation. For siloxanes, begin polyatomic gases, vibrational relaxation is the main point of concern, since contrary to translational and rotational equilibrium, which is achieved in only few collisions, the achievement of vibrational equilibrium may require thousands of collisions.[57] Moreover, polyatomic gases have several modes of molecular vibration—each of which can, in principle, relax independently—and are structurally flexible. Consequently, they can change their shape, both during normal vibration and during collision, the latter being probably more relevant. The majority of polyatomic gases exhibit a single vibrational relaxation process, which involves the entire vibrational energy content of the molecule. This is based on the assumption that vibrational-vibrational energy transfer is faster than vibrational-translational; therefore, the total vibrational energy content of a molecule relaxes by vibrational-translational energy transfer via the lowest mode. For estimating the vibrational relaxation time, the mode of the lowest frequency of vibration is required. These data were determined from *ab initio*

TABLE IV. $\Gamma_{\min}$ along the dew-line. Values are calculated by increasing and decreasing the accepted value of C_P^0 by 5% to assess the influence on Γ.

	$\Gamma_{\min}^V$	
Fluid	$C_P^0+5\%$	$C_P^0-5\%$
MDM	0.048	0.123
MD_2M	0.038	0.110
MD_3M	−0.130	−0.049
MD_4M	−0.129	−0.042
D_4	0.067	0.133
D_5	0.016	0.085
D_6	−0.270	−0.170

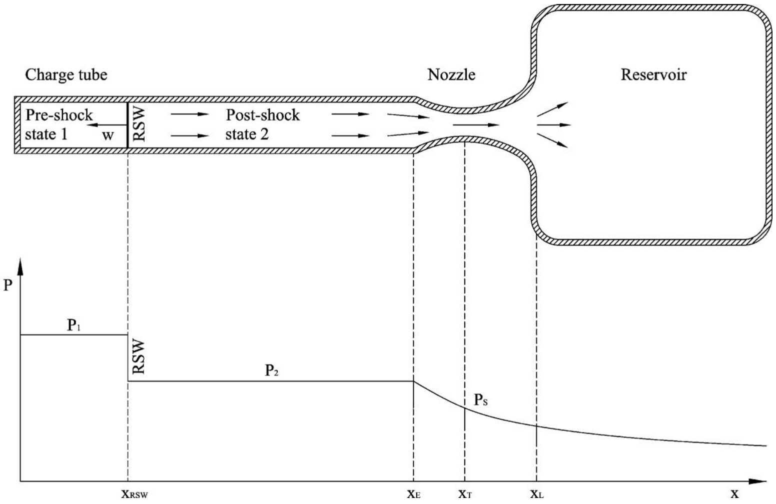

FIG. 6. Schematic representation of the Ludwieg tube adopted for the simulation of the propagation of a rarefaction shock wave.

calculations, as treated in Ref. 41. The computed lowest frequency of vibration for all the siloxanes considered here is lower than 40 cm^{-1}. By using the Lambert-Salter plot (see Ref. 58) for molecules containing more than two hydrogen atoms, the vibrational relaxation time is estimated to be of the order of 0.1 ns; i.e., 10^{-10} s at 300 K. The fact that the pre- and postshock states for rarefaction shocks are at a higher pressure and temperature, should not have a significant effect on the estimation of the order of magnitude of the vibrational relaxation time.[57] As in Ref. 22, the rarefaction shock thickness for D_6 can be computed based on: (i) the calculated viscosity using the method of Chung *et al.*, (ii) the assumption that the bulk viscosity is of the same order of magnitude as the shear viscosity, and (iii) that the ratio of the isobaric with respect to the isochoric heat capacity is of the order of 1. This results in an estimated shock thickness of the order of micrometers and therefore the residence time of the molecule—for a speed of sound of about 40 m/s—is of the order of 10^{-8} s. According to these calculations, the relaxation time is at least two orders of magnitude smaller than the residence time of a molecule in the shock. Equilibrium of the internal energy can therefore be assumed past the shock wave.

IV. CONCLUSIONS

This paper provides a critical overview of the families of fluids that can exhibit nonclassical gasdynamic behavior as well as the results of calculations of Γ for siloxanes employing a state-of-the-art thermodynamic model. Due to the high sensitivity of the value of Γ to the accuracy of the calculation of primary thermodynamic properties, the adoption of a highly accurate equation of state is deemed mandatory.

According to the adopted thermodynamic model, i.e., equations of state in the Span-Wagner functional form, several fluids of the siloxanes class, namely, D_6, MD_3M, and MD_4M, exhibit a thermodynamic region where the fundamental derivative of gasdynamics is negative. However, uncertainties in the estimation of Γ remain large and difficult to estimate, because experimental data for these complex molecules are still scarce, especially in the region of interest.

Additional work in this respect will involve the investigation of the influence of global critical phenomena in the dense-gas region where the nonclassical phenomena are predicted and possibly the computation of P-v-T data by means of molecular dynamics or Monte Carlo simulations. In order to obtain insight in the suitability of equations of state to

TABLE V. Properties of the pre- and postshock fluid states of the rarefaction shock wave illustrated in Fig. 7 and thermodynamic states in the throat of the nozzle. The ratio of the area of the throat with respect to the area of the pipe is 0.4196, *w* is the flow velocity with respect to a frame of reference moving with the shock. *u* represents the flow velocity with respect to a stationary observer.

Property		Preshock state		Postshock state		Nozzle throat	
		Numerical	Analytical	Numerical	Analytical	Numerical	Analytical
P	[kPa]	912.62	912.62	800.26	801.17	557.83	557.43
T	[°C]	369.19	369.19	364.12	364.05	357.78	357.36
ρ	[m^3/kg]	186.11	186.11	127.01	127.54	67.74	67.82
w	[m/s]	36.02[a]	36.12[a]	52.78	52.70	—	—
c	[m/s]	35.22	35.22	52.95	52.70	75.11	74.96
u	[m/s]	0.00	0.00	16.76	16.58	75.01	74.96
Ma	[-]	1.023 3[b]	1.026[b]	0.997[b]	1.000[b]	0.999[c]	1.000[c]

[a] The speed of the rarefaction shock is 36.02 m/s, moving to the left (see Fig. 6).

[b] Ma number with respect to a shock related frame of reference.

[c] Ma number with respect to a laboratory frame of reference.

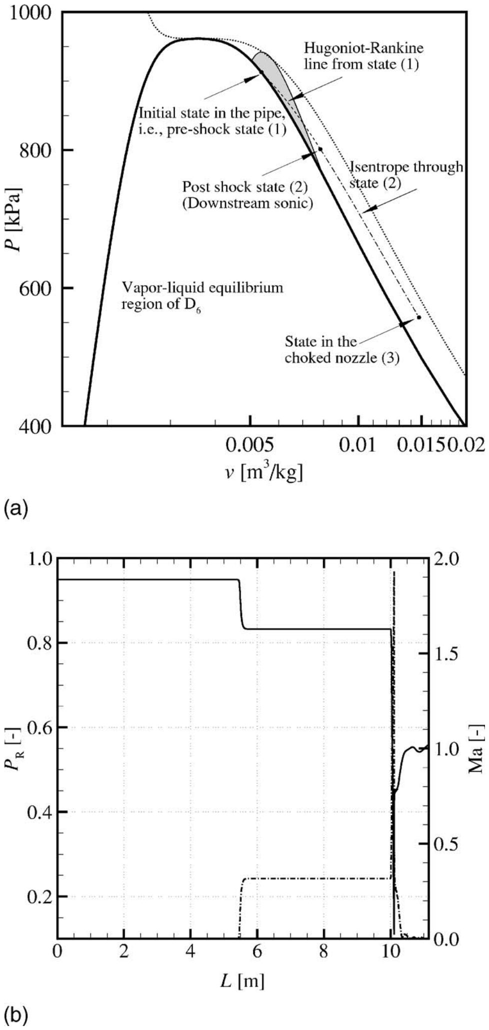

FIG. 7. (a) Thermodynamic states in the P-v plane characterizing a rarefaction shock wave propagating in fluid D$_6$. Note that at state (2) the Hugoniot-Rankine line from state (1) and the Rayleigh line through states (1) and (2) are tangent. The ratio of the area of the throat and that of the pipe is such that the wave is purely expansive, therefore avoiding the formation of a rarefaction fan as a tail. (b) Variation of pressure (solid line) and Mach number (dash-dot line) (with respect to a stationary frame of reference; i.e., $\mathrm{Ma}=u/c$) at $t\approx 130$ ms. The Mach number at the postshock state is sonic, i.e., $\mathrm{Ma}_2=1.0$, with respect to a frame of reference moving with the simulated rarefaction shock wave. Remark that $P_R=P/P_{\mathrm{ref}}$, where $P_{\mathrm{ref}}=961.366$ kPa (Ref. 31).

estimate Γ, work is underway to analyze the computation of Γ for several lighter fluids of the class of n-alkanes. Even though none of them is expected to classify as a BZT fluid, the availability of accurate measurements in the close-to-critical region and therefore the use of reliable reference equations of state will possibly allow for an estimation of the uncertainty in the calculation of the fundamental derivative of gasdynamics.

ACKNOWLEDGMENTS

This research is supported by the Dutch Technology Foundation STW, Applied Science Division of NWO, and the Technology Program of the Ministry of Economic Affairs, Grant No. DSF.6573.

APPENDIX: RELEVANT EXPRESSIONS FOR COMPUTING THE FUNDAMENTAL DERIVATIVE FROM A CANONICAL HELMHOLTZ FUNCTION

For the computation of the fundamental derivative and other thermodynamic properties, first-order, second-order, and composite derivatives of pressure with respect to specific volume and temperature are required. Expressions for the computation of main thermodynamic functions from a canonical Helmholtz EoS are presented in the following. The Helmholtz function can be formulated as $\Psi(T,\rho)/(RT)=[\psi^0(\tau,\delta)+\psi^{\mathrm{r}}(\tau,\delta)]$, where $\delta\equiv\rho/\rho_c=v_c/v$, and $\tau=T_c/T$. The ideal-gas part of the Helmholtz function is

$$\psi^0(\tau,\delta)=\frac{h_0^0\tau}{RT_c}-\frac{s_0^0}{R}-1+\ln\left(\frac{\tau_0\delta}{\delta_0\tau}\right)-\frac{\tau}{R}\int_{\tau_0}^{\tau}\frac{C_P^0}{\tau^2}d\tau+\frac{1}{R}\int_{\tau_0}^{\tau}\frac{C_P^0}{\tau}d\tau, \tag{A1}$$

where $\delta_0=\rho_0/\rho_c$ and $\tau_0=T_c/T_0$ and represent the reduced density and the inverse of the reduced temperature, respectively at a predefined or prescribed reference state (T_0,ρ_0). Hence,

$$\frac{Pv}{RT}=Z=1+\delta\left(\frac{\partial\psi^{\mathrm{r}}}{\partial\delta}\right)_{\tau}. \tag{A2}$$

The values of h_0^0 and s_0^0 (at the reference temperature T_0 and volume v_0) are chosen based on recommendations of the International Union of Pure and Applied Chemistry (IUPAC) or according to conventions used in industry.

The pressure derivatives are computed as

$$\left(\frac{\partial P}{\partial v}\right)_T=-\frac{RT}{v^2}\left[1+2\delta\left(\frac{\partial\psi^{\mathrm{r}}}{\partial\delta}\right)_{\tau}+\delta^2\left(\frac{\partial^2\psi^{\mathrm{r}}}{\partial\delta^2}\right)_{\tau}\right], \tag{A3}$$

$$\left(\frac{\partial P}{\partial T}\right)_v=\frac{R}{v}\left[1+\delta\left(\frac{\partial\psi^{\mathrm{r}}}{\partial\delta}\right)_{\tau}-\delta\tau\left(\frac{\partial^2\psi^{\mathrm{r}}}{\partial\tau\partial\delta}\right)_{\tau,\delta}\right], \tag{A4}$$

$$\left(\frac{\partial^2 P}{\partial v^2}\right)_T=\frac{RT}{v^3}\left[2+6\delta\left(\frac{\partial\psi^{\mathrm{r}}}{\partial\delta}\right)_{\tau}+6\delta^2\left(\frac{\partial^2\psi^{\mathrm{r}}}{\partial\delta^2}\right)_{\tau}+\delta^3\left(\frac{\partial^3\psi^{\mathrm{r}}}{\partial\delta^3}\right)_{\tau}\right], \tag{A5}$$

$$\left(\frac{\partial^2 P}{\partial T\partial v}\right)=\frac{R}{v^2}\left\{\tau\delta\left[2\left(\frac{\partial^2\psi^{\mathrm{r}}}{\partial\tau\partial\delta}\right)_{\delta,\tau}+\delta\left(\frac{\partial^3\psi^{\mathrm{r}}}{\partial\tau\partial^2\delta}\right)_{\delta,\tau}\right]-\left[1+2\delta\left(\frac{\partial\psi^{\mathrm{r}}}{\partial\delta}\right)_{\tau}+\delta^2\left(\frac{\partial^2\psi^{\mathrm{r}}}{\partial\delta^2}\right)_{\tau}\right]\right\}, \tag{A6}$$

$$\left(\frac{\partial^2 P}{\partial T^2}\right)_v=\frac{R}{Tv}\left[\delta\tau^2\left(\frac{\partial^3\psi^{\mathrm{r}}}{\partial\tau^2\partial\delta}\right)_{\tau,\delta}\right], \tag{A7}$$

and the isochoric specific heat and its first order derivative with respect to the temperature read

$$C_v=-R\tau^2\left[\left(\frac{\partial^2\psi^0}{\partial\tau^2}\right)_{\delta}+\left(\frac{\partial^2\psi^{\mathrm{r}}}{\partial\tau^2}\right)_{\delta}\right], \tag{A8}$$

$$\left(\frac{\partial C_v}{\partial T}\right)_v = \frac{R\tau}{T}\left[2\tau\left(\frac{\partial^2 \psi^0}{\partial \tau^2}\right)_\delta + 2\tau\left(\frac{\partial^2 \psi^r}{\partial \tau^2}\right)_\delta + \tau^2\left(\frac{\partial^3 \psi^0}{\partial \tau^3}\right)_\delta + \tau^2\left(\frac{\partial^3 \psi^r}{\partial \tau^3}\right)_\delta\right]. \tag{A9}$$

In the expressions above, according to the Span-Wagner functional form, the residual part of the Helmholtz function is computed as follows:

$$\begin{aligned}\psi^r(\tau,\delta) &= n_1\delta\tau^{0.250} + n_2\delta\tau^{1.125} + n_3\delta\tau^{1.500} + n_4\delta^2\tau^{1.375} \\ &\quad + n_5\delta^3\tau^{0.250} + n_6\delta^7\tau^{0.875} + n_7\delta^2\tau^{0.625}e^{-\delta} \\ &\quad + n_8\delta^5\tau^{1.750}e^{-\delta} + n_9\delta\tau^{3.625}e^{-\delta^2} + n_{10}\delta^4\tau^{3.625}e^{-\delta^2} \\ &\quad + n_{11}\delta^3\tau^{14.5}e^{-\delta^3} + n_{12}\delta^4\tau^{12.0}e^{-\delta^3},\end{aligned} \tag{A10}$$

where the coefficients $n_1 \cdots n_{12}$ depend on the fluid.

[1] R. Menikoff and B. J. Plohr, "The Riemann problem for fluid flow of real material," Rev. Mod. Phys. **61**, 75 (1989).

[2] W. D. Hayes, "The basic theory of gasdynamic discontinuities," in *Fundamentals of Gas Dynamics*, High Speed Aerodynamics and Jet Propulsion Vol. 3, edited by H. W. Emmons (Princeton University Press, Princeton, NJ, 1958).

[3] P. A. Thompson, *Compressible Fluid Dynamics* (McGraw-Hill, New York, 1988).

[4] Ya. B. Zel'dovich and Yu. P. Raizer, *Physics of Shock Waves and High-Temperature Hydrodynamic Phenomena* (Academic New York, 1966), Vol. 1.

[5] Y. B. Zel'dovich, *Theory of Shock Waves and Introduction to Gas Dynamics* (Izdatel'stvo Akademii Nauk SSSR, Moscow, 1946).

[6] See National Technical Information Service Document No. PB 032189 (H. A. Bethe, "The theory of shock waves for an arbitrary equation of state," Office of Scientific Research and Development Paper No. 545, 1942). Copies may be ordered from the National Technical Information Service, Springfield, VA.

[7] P. A. Thompson, "A fundamental derivative in gasdynamics," Phys. Fluids **14**, 1843 (1971).

[8] M. S. Cramer and A. Kluwick, "On the propagation of waves exhibiting both positive and negative nonlinearity," J. Fluid Mech. **142**, 9 (1984).

[9] M. S. Cramer, "Structure of weak shocks in fluids having embedded regions of negative nonlinearity," Phys. Fluids **30**, 3034 (1987).

[10] M. S. Cramer and R. Sen, "Exact solutions for sonic shocks in Van der Waals gases," Phys. Fluids **30**, 377 (1987).

[11] M. S. Cramer and R. Sen, "Shock formation in fluids having embedded regions of negative nonlinearity," Phys. Fluids **29**, 2181 (1986).

[12] P. Colonna and A. Guardone, "Molecular interpretation of nonclassical gas dynamics of dense vapors under the Van der Waals model," Phys. Fluids **18**, 056101 (2006).

[13] A. G. Ivanov and S. A. Novikov, "Rarefaction shock waves in iron and steel," Zh. Eksp. Teor. Fiz. **40**, 1880 (1961).

[14] A. A. Borisov, Al. A. Borisov, S. S. Kutateladze, and V. E. Nakoryakov, "Rarefaction shock wave near the critical liquid-vapor point," J. Fluid Mech. **126**, 59 (1983).

[15] S. S. Kutateladze, V. E. Nakoryakov, and A. A. Borisov, "Rarefaction waves in liquid and gas-liquid media," Annu. Rev. Fluid Mech. **19**, 577 (1987).

[16] B. S. Fergason, T. L. Ho, B. M. Argrow, and G. Emanuel, "Theory for producing a single-phase rarefaction shock wave in a shock tube," J. Fluid Mech. **445**, 37 (2001).

[17] A. A. Borisov, Al. A. Borisov, and V. E. Nakoryakov, *Adiabatic Waves in Liquid-Vapor Systems* (Springer-Verlag, Berlin, 1990). pp. 239–245.

[18] P. A. Thompson, G. C. Carofano, and Y. Kim, "Shock waves and phase changes in a large-heat-capacity fluid emerging from a tube," J. Fluid Mech. **166**, 57 (1986).

[19] S. Fergason, A. Guardone, and B. Argrow, "Construction and validation of a dense gas shock tube," J. Thermophys. Heat Transfer **17**, 326 (2003).

[20] S. Fergason, "Dense gas shock tube," Ph.D. thesis, Aerospace Engineering Sciences Department, University of Colorado, Boulder, CO, 2001.

[21] K. C. Lambrakis and P. A. Thompson, "Existence of real fluids with negative fundamental derivative," Phys. Fluids **15**, 933 (1972).

[22] P. A. Thompson and K. C. Lambrakis, "Negative shock waves," J. Fluid Mech. **60**, 187 (1973).

[23] M. S. Cramer, "Negative nonlinearity in selected fluorocarbons," Phys. Fluids A **1**, 1894 (1989).

[24] P. Colonna and P. Silva, "Dense gas thermodynamic properties of single and multi-component fluids for fluid dynamics simulations," J. Fluids Eng. **125**, 414 (2003).

[25] A. Guardone and B. M. Argrow, "Nonclassical gasdynamic region of selected fluorocarbons," Phys. Fluids **17**, 116101 (2005).

[26] I. Obernberger, P. Thonhofer, and E. Reisenhofer, "Description and evaluation of the new 1,000 kW$_{\mathrm{el}}$ organic Rankine cycle process integrated in the biomass CHP plant in Lienz, Austria," Euroheat and Power **2**, 1 (2001).

[27] G. Angelino and P. Colonna, "Multicomponent working fluids for organic Rankine cycles (ORCs)," Energy **23**, 449 (1998).

[28] G. Angelino and P. Colonna, "Air cooled siloxane bottoming cycle for molten carbonate fuel cells," in *2000 Fuel Cell Seminar*, Portland, Oregon, October 30–November 2, 2000, No. 114, pp. 667–670.

[29] G. Angelino and P. Colonna, "Organic Rankine cycles for energy recovery from molten carbonate fuel cells," in 35th Intersociety Energy Conversion Engineering (IECEC) Conference and Exhibit, Reston, VA, July 2000, AIAA Paper No. 2000-3052.

[30] B. P. Brown and B. M. Argrow, "Application of Bethe-Zel'dovic-Thompson fluids in organic Rankine cycle engines," J. Propul. Power **16**, 1118 (2000).

[31] P. Colonna and S. Rebay, "Numerical simulation of dense gas flows on unstructured grids with an implicit high resolution upwind Euler solver," Int. J. Numer. Methods Fluids **46**, 735 (2004).

[32] J. F. Monaco, M. S. Cramer, and L. T. Watson, "Supersonic flows of dense gases in cascade configurations," J. Fluid Mech. **330**, 31 (1997).

[33] G. H. Schnerr and P. Leidner, "Numerical investigation of axial cascades for dense gases," in *PICAST'1-Pacific International Conference on Aerospace Science Technology*, Taiwan, December 1993, edited by E. L. Chin (National Cheng Kung University, Taiwan, 1994), Vol. 2, pp. 818–825.

[34] A. Guardone, L. Vigevano, and B. M. Argrow, "Assessment of thermodynamic models for dense gas dynamics," Phys. Fluids **16**, 3878 (2004).

[35] R. Span and W. Wagner, "Equations of state for technical applications I. Simultaneously optimized functional forms for nonpolar and polar fluids," Int. J. Thermophys. **24**, 1 (2003).

[36] P. Colonna, N. R. Nannan, A. Guardone, and E. W. Lemmon, "Multiparameter equations of state for selected siloxanes," Fluid Phase Equilib. **244**, 193 (2006).

[37] D. Y. Peng and D. B. Robinson, "A new two-constant equation of state," Ind. Eng. Chem. Fundam. **15**, 59 (1976).

[38] R. Stryjek and J. H. Vera, "PRSV, An improved Peng-Robinson equation of state for pure compounds and mixtures," Can. J. Chem. Eng. **64**, 323 (1986).

[39] P. Colonna, "Fluidi di Lavoro Multi Componenti Per Cicli Termodinamici di Potenza (Multicomponent working fluids for power cycles)," Ph.D. thesis, Politecnico di Milano, October 1996.

[40] G. Angelino and C. Invernizzi, "Cyclic methylsiloxanes as working fluids for space power cycles," J. Sol. Energy Eng. **115**, 130 (1993).

[41] N. R. Nannan, P. Colonna, C. M. Tracy, R. L. Rowley, and J. J. Hurly, "Ideal-gas heat capacities of dimethylsiloxanes from speed-of-sound measurements and ab initio calculations," Fluid Phase Equilib. **257**, 102 (2007).

[42] B. M. Argrow, "Computational analysis of dense gas shock tube flow," Shock Waves **6**, 241 (1996).

[43] P. Cinnella and P. Congedo, "A numerical solver for dense gas flows," in 34th AIAA Fluid Dynamics Conference and Exhibit, June–July 2004, AIAA Paper No. 2004-2137, pp. 1–12.

[44] P. Cinnella and P. M. Congedo, "Aerodynamic performance of transonic Bethe-Zel'dovich-Thompson flows past an airfoil," AIAA J. **43**, 370 (2005).

[45] A. Guardone and L. Vigevano, "Roe linearization for the Van der Waals gas," J. Comput. Phys. **175**, 50 (2002).

[46] B. P. Brown and B. M. Argrow, "Two-dimensional shock tube flow for dense gases," J. Fluid Mech. **349**, 95 (1997).

[47] C. Zamfirescu, A. Guardone, and P. Colonna, "Numerical simulation of the FAST dense gas experiment," in *European Conference on Computational Fluid Dynamics ECCOMAS 2006*, edited by P. Wesseling, E. Oñate, and J. Périaux (TU, Delft, 2006), p. 17.

[48] C. Zamfirescu, A. Guardone, and P. Colonna, "Preliminary design of the

FAST dense gas Ludwieg tube," in *9th AIAA/ASME Joint Thermophysics and Heat Transfer Conference*, San Francisco, CA, June 2006 (American Institute of Aeronautics and Astronautics, Reston, VA, 2006), AIAA Paper No. 2006–3249, pp. 1–14.

[49] G. Emanuel, "Assessment of the Martin-Hou equation for modeling a nonclassical fluid," J. Fluids Eng. **116**, 883 (1994).

[50] E. C. Ihmels, "Helmholtz type fundamental equations of state-some practice applications," in Thermo International 2006: Sixteenth Symposium on Thermophysical Properties, July–August 2006, National Institute of Standards and Technology, pp. 1–11.

[51] J. J. Martin and Y. C. Hou, "Development of an equation of state for gases," AIChE J. **1**, 142 (1955).

[52] R. L. Rowley, W. V. Wilding, J. L. Oscarson, Y. Yang, N. A. Zundeland, T. P. Daubert, and R. P. Danner, *DIPPR Data Compilation of Pure Chemical Properties* (Taylor & Francis, New York, 2004).

[53] N. R. Nannan, J. J. Hurly, and P. Colonna, "Speed of sound and ideal-gas heat capacity data for selected siloxanes from acoustic measurements: $[(CH_3)_2-Si-O]_4$ and $[(CH_3)_2-Si-O]_5$," in Thermo International 2006: Sixteenth Symposium on Thermophysical Properties, July–August 2006, edited by G. Hardin, C. Muzny, and D. Friend, National Institute of Standards and Technology, pp. 1–19.

[54] I. I. Glass and J. P. Sislian, *Nonstationary Flows and Shock Waves* (Clarendon, Oxford, 1994).

[55] H. Mirels, "Laminar boundary layer behind shock advancing into stationary fluid," Technical Note TN 3401, National Advisory Committee for Aeronautics, March 1955.

[56] T.-H. Chung, M. Ajlan, L. L. Lee, and K. E. Starling, "Generalized multiparameter correlation for non-polar and polar fluid transport properties," Ind. Eng. Chem. Res. **27**, 671 (1988).

[57] J. D. Lambert, *Vibrational and Rotational Relaxation in Gases*, The International Series of Monographs on Chemistry (Clarendon, Oxford, 1977).

[58] J. D. Lambert, *Vibrational and Rotational Relaxation in Gases*, The International Series of Monographs on Chemistry (Clarendon, Oxford, 1977), Chap. 3, p. 64.

[59] B. E. Poling, J. M. Prausnitz, and J. P. O'Connell, *The Properties of Gases and Liquids*, Chemical Engineering Series, 5th ed. (McGraw-Hill, New York, 2001).

[60] D. D. Lindley and H. C. Hershey, "The orthobaric region of octamethyltrisiloxane," Fluid Phase Equilib. **55**, 109 (1990).

[61] C. B. Hurd, "Studies of siloxanes. I. The specific volume and viscosity in relation to temperature and constitution," J. Am. Chem. Soc. **68**, 364 (1946).

[62] O. L. Flaningam, "Vapor pressures of poly(dimethylsiloxane) oligomers," J. Chem. Eng. Data **31**266 (1986).

[63] I. I. Skorokhodov, V. E. Ditsent, N. A. Terentéva, and M. N. Zolotareva, "Pressure of the saturated vapor of polydiorganosiloxane. 1. Polydimetylsiloxane," Deposited Document No. VINITI N2725–71, All-Russian Institute of Scientific and Technical Information of the Russian Academy of Sciences—Vserossiisky Institut Nauchnoi i Tekhnicheskoi Informatsii (VINITI), 1971, p. 11.

[64] D. H. Marcos, D. D. Lindley, K. S. Wilson, W. B. Kay, and H. C. Hershey, "A (P,v,T) study of tetramethylsilane, hexamethyldisiloxane, octamethyltrisiloxane, and toluene from 423 K to 573 K in the vapor phase," J. Chem. Thermodyn. **15**, 1003 (1983).

[65] I. A. McLure, A. J. Pretty, and P. A. Sadler, "Specific volumes, thermal pressure coefficients, and derived quantities of five dimethylsiloxane oligomers from 25 to 140 °C," J. Chem. Eng. Data **22**, 372 (1977).